



OPEN

Doubling of annual forest carbon loss over the tropics during the early twenty-first century

Yu Feng^{1,2}, Zhenzhong Zeng¹✉, Timothy D. Searchinger³, Alan D. Ziegler⁴, Jie Wu^{1,5}, Dashan Wang¹, Xinyue He^{1,6}, Paul R. Elsen⁷, Philippe Ciais^{8,9}, Rongrong Xu¹, Zhilin Guo¹, Liqing Peng¹⁰, Yiheng Tao¹¹, Dominick V. Spracklen⁶, Joseph Holden¹², Xiaoping Liu¹³, Yi Zheng¹, Peng Xu¹, Ji Chen¹✉, Xin Jiang¹, Xiao-Peng Song¹⁴, Venkataraman Lakshmi¹⁵, Eric F. Wood¹¹ and Chunmiao Zheng¹✉

Previous estimates of tropical forest carbon loss in the twenty-first century using satellite data typically focus on its magnitude, whereas regional loss trajectories and associated drivers are rarely reported. Here we used different high-resolution satellite datasets to show a doubling of gross tropical forest carbon loss worldwide from $0.97 \pm 0.16 \text{ PgC yr}^{-1}$ in 2001–2005 to $1.99 \pm 0.13 \text{ PgC yr}^{-1}$ in 2015–2019. This increase in carbon loss from forest conversion is higher than in bookkeeping models forced by land-use statistical data, which show no trend or a slight decline in land-use emissions in the early twenty-first century. Most (82%) of the forest carbon loss is at some stages associated with large-scale commodity or small-scale agriculture activities, particularly in Africa and Southeast Asia. We find that ~70% of former forest lands converted to agriculture in 2001–2019 remained so in 2020, confirming a dominant role of agriculture in long-term pan-tropical carbon reductions on formerly forested landscapes. The acceleration and high rate of forest carbon loss in the twenty-first century suggest that existing strategies to reduce forest loss are not successful; and this failure underscores the importance of monitoring deforestation trends following the new pledges made in Glasgow.

Fossil fuel carbon emissions, oceanic carbon sinks and atmospheric carbon dioxide growth rates have been quantified reasonably well in global carbon cycle analyses; however, estimates of land carbon sinks/sources still have large uncertainties^{1–3}. Further, the trends in global land-use-change emissions are uncertain in the global carbon budget¹, with results averaged from three bookkeeping models showing either increases or decreases in land-use emissions in the past decade^{1,4}. In addition, the *Global Carbon Budget 2021*¹ suggests a negative imbalance between sources and sinks, whereas the *Global Carbon Budget 2019*⁵ shows a positive imbalance. The contradictory trends in land-use-change emissions from different bookkeeping models result from differences in input land-use data, demonstrating the need for more accurate estimates to address the persistent uncertainty in closing the global carbon budget.

The net land carbon flux is the most uncertain component of the global carbon budget^{2,3}. Deforestation in the tropics, currently the hotspot of global forest carbon loss^{6–8}, directly releases carbon stored in vegetation and soil and indirectly decreases the carbon sink capacity of terrestrial ecosystems^{9–11}. Large uncertainties exist in the spatiotemporal pattern of tropical forest loss and associated carbon stock changes in the twenty-first century^{12,13}, such that the

contribution of tropical forest ecosystems to the global carbon budget is contested^{12–14}. Spatially explicit quantification of tropical forest carbon loss and its trajectory greatly helps reduce uncertainties and ascertain the contribution of tropical forest ecosystems to the global carbon budget over time.

In this article, we analyse gross forest carbon loss associated with forest removal over the tropics (between 23.5°N and 23.5°S but excluding northern Australia) during the twenty-first century. We quantify regional fluxes and trends, as well as examine the drivers of change and the fate of transitioning land uses following forest loss in an effort to gain insights on the permanence of forest conversion to other land-use types. Our analysis co-locates high-spatiotemporal-resolution forest loss from the Global Forest Change (GFC) product¹⁵ (annual data at 30 m spatial resolution) with corresponding values of forest (aboveground and belowground) biomass carbon and soil organic carbon (SOC). The GFC product was created using different algorithms and satellite data during the study period, potentially resulting in temporal inconsistencies^{16,17}. To address this issue, we use a stratified random-sample approach¹⁸ to analyse forest loss area trends, following the recommendation of the Global Forest Watch¹⁹. Different from existing studies^{7–9,12,20}, our analysis is based on the quantification of forest loss area using a

¹State Environmental Protection Key Laboratory of Integrated Surface Water–Groundwater Pollution Control, School of Environmental Science and Engineering, Southern University of Science and Technology, Shenzhen, China. ²Department of Civil Engineering, The University of Hong Kong, Hong Kong, China. ³School of Public and International Affairs, Princeton University, Princeton, NJ, USA. ⁴Faculty of Fisheries Technology and Aquatic Resources, Mae Jo University, Chiang Mai, Thailand. ⁵Department of Geoscience and Natural Resource Management, University of Copenhagen, Copenhagen, Denmark. ⁶School of Earth and Environment, University of Leeds, Leeds, UK. ⁷Wildlife Conservation Society, Global Conservation Program, Bronx, NY, USA. ⁸Laboratoire des Sciences du Climat et de l'Environnement, UMR 1572 CEA-CNRS-UVSQ, Gif-sur-Yvette, France. ⁹Climate and Atmosphere Research Center (CARE-C), The Cyprus Institute, Nicosia, Cyprus. ¹⁰World Resources Institute, Washington, DC, USA. ¹¹Department of Civil and Environmental Engineering, Princeton University, Princeton, NJ, USA. ¹²School of Geography, University of Leeds, Leeds, UK. ¹³School of Geography and Planning, Sun Yat-Sen University, Guangzhou, China. ¹⁴Department of Geosciences, Texas Tech University, Lubbock, TX, USA. ¹⁵Department of Engineering Systems and Environment, University of Virginia, Charlottesville, VA, USA. ✉e-mail: zengzz@sustech.edu.cn; jichen@hku.hk; zhengcm@sustech.edu.cn

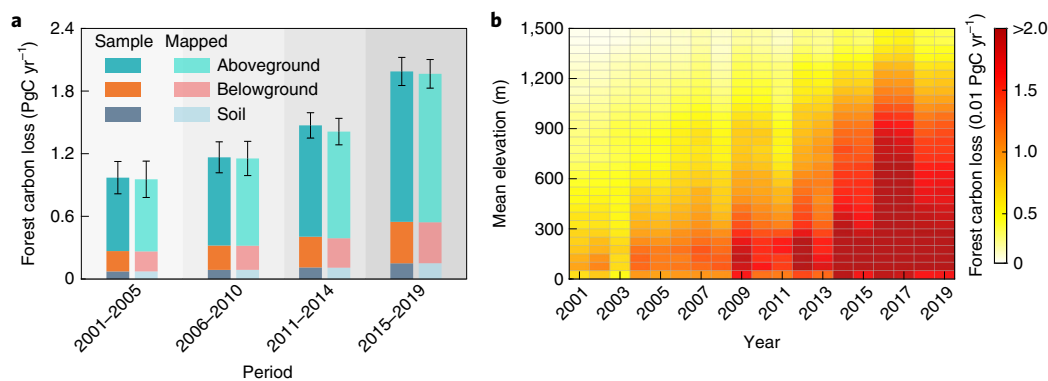


Fig. 1 | Forest carbon loss across the tropics during 2001–2019. **a**, Forest carbon loss during different subperiods. Four grouped bars (left to right) show mean annual forest carbon loss during the four periods of 2001–2005, 2006–2010, 2011–2014 and 2015–2019, respectively. Error bars represent the s.d. of total forest carbon loss (including losses aboveground, belowground and from the soil) estimated by four carbon density maps. Sample bars show that mean annual forest carbon loss for the last five years (2015–2019, 1.99 PgC yr^{-1}) is 2.1 times as large as that for the beginning of the twenty-first century (2001–2005, 0.97 PgC yr^{-1}). **b**, Increasing carbon loss resulting from tropical mountain forest loss in elevation–year space. Forest carbon loss includes aboveground and (committed) belowground biomass carbon loss and (committed) soil organic carbon loss.

stratified random-sample approach and of forest carbon loss using a ‘stratify and multiply’ approach^{21,22}. Belowground biomass and soil carbon losses occur in nature as a transient legacy of forest aboveground carbon loss, but they are presented here as committed losses. Further, we assess the spatiotemporal dynamics of forest carbon loss, the different drivers of forest transitions and the permanence of land-use types established after forest loss. Our estimates of gross carbon losses ignore partial carbon recovery in secondary forests and plantations; and they cover all activities that result in forest cover loss, including both natural and anthropogenic disturbances.

Patterns of forest carbon loss

Overall, the stratified random-sample estimate of mean annual carbon loss from tropical forest conversion is $1.39 \pm 0.14 \text{ PgC yr}^{-1}$ during 2001–2019 (Fig. 1a). This estimate includes an aboveground shoot biomass carbon loss of $1.01 \pm 0.11 \text{ PgC yr}^{-1}$ (73%), a belowground root biomass committed carbon loss of $0.28 \pm 0.03 \text{ PgC yr}^{-1}$ (20%) and a SOC committed loss of 0.10 PgC yr^{-1} (7%). We find that mean annual tropical forest carbon loss during the last five years of our analysis (2015–2019, $1.99 \pm 0.13 \text{ PgC yr}^{-1}$; Fig. 1a) has more than doubled from that of the first five years of the twenty-first century (2001–2005, $0.97 \pm 0.16 \text{ PgC yr}^{-1}$). The increase in aboveground carbon loss dominates this doubling of the total loss (72% , $0.74 \pm 0.06 \text{ PgC yr}^{-1}$), followed by belowground committed carbon loss (20% , $0.20 \pm 0.02 \text{ PgC yr}^{-1}$) and SOC committed loss (8% , 0.08 PgC yr^{-1}). Throughout the study period, annual forest carbon loss significantly increased at a rate of $0.60^{+0.21}_{-0.10} \text{ PgC yr}^{-1} \text{ decade}^{-1}$ (subscript and superscript values give the 95% confidence interval; Mann–Kendall test; $P < 0.01$). We further find that 22% of the total tropical forest carbon loss occurred in the mountains during the 19 yr study period (Fig. 1b), even though they represent only 17.8% of the whole tropical land areas. Mountain areas contribute 33% of the doubling in tropical forest carbon loss, indicating a clear acceleration in mountain forest carbon loss²³. In particular, mountain forests in tropical Asia, which have relatively high biomass carbon stocks^{23,24} (Supplementary Fig. 1), have experienced high rates of conversion during the past two decades. These trends have not been explicitly incorporated in recent assessments, including the Intergovernmental Panel on Climate Change Sixth Assessment Report⁶.

The spatial pattern of changes in annual forest carbon loss varies regionally (Fig. 2). Since 2001, annual forest carbon loss increased significantly and continuously over tropical Africa and

Asia ($P < 0.01$), accounting for 38% and 43% of the increase in pan-tropical carbon loss, respectively (Supplementary Fig. 2). In Africa, annual forest carbon loss sharply increased in the Congo basin (for example, Democratic Republic of the Congo (D. R. Congo) and Cameroon), Angola and some countries to the north on the west African coast (for example, Guinea, Ivory Coast and Liberia) during 2015–2019 (Table 1). Parts of Southeast Asia (SEA), particularly Peninsular Malaysia, Sabah state and some Indonesian islands, are lingering hotspots of forest carbon loss²⁵. More recently, forest carbon loss increased quickly in northern parts of montane mainland SEA (Fig. 2 and Table 1). By contrast, the trend in forest carbon loss over tropical America during 2001–2019 is not significant ($P > 0.05$), even though losses are locally high in some areas. For example, during 2001–2005, most forest carbon loss occurred between the Cerrado and Amazonian biomes in Brazil, in the area known as the Arc of Deforestation (Fig. 2a). During 2015–2019, forest carbon loss declined in southeastern Amazonian regions of Brazil, including the Mato Grosso and Rondônia states, but increased in the central Para and Maranhão states. Increases also occurred in southeast Bolivia, central Peru, Mexico and Central America (Fig. 2b,c). Annual forest carbon loss over tropical America reached its highest levels during 2016–2017, occurring mostly in Amazonia (Supplementary Fig. 3a–c). It was once projected that Brazil would halve deforestation rates by 2020, on the basis of data from 2001 to 2013²⁰. However, our updated analysis shows a reversal and a new increase in Brazil’s forest carbon loss after 2015. Our reported trend in forest carbon loss during the 2010s in Brazil is in agreement with forest area change observed in the Brazilian Amazon using a different methodology²⁶, further confirming the increase in forest carbon loss in the region since 2015 and demonstrating that our results are robust to the choice of a forest loss algorithm¹⁷.

Drivers of forest carbon loss

By combining our results with a map of forest loss drivers²⁷, we find that the conversion of forest to some types of agricultural land dominates forest carbon loss in all three continents, but geographical differences do occur over time (Fig. 3). In tropical America, much of the lands replacing forest are large-scale commodity agriculture operations, including rangelands for beef, and croplands for oilseeds and cereals (Fig. 3b). In Brazil (Fig. 3e), for example, commodity-driven conversions decreased sharply from 2004 to 2009, remained stable during 2010–2014 and substantially increased afterwards. Small-scale agriculture (including various forms of shifting agriculture)

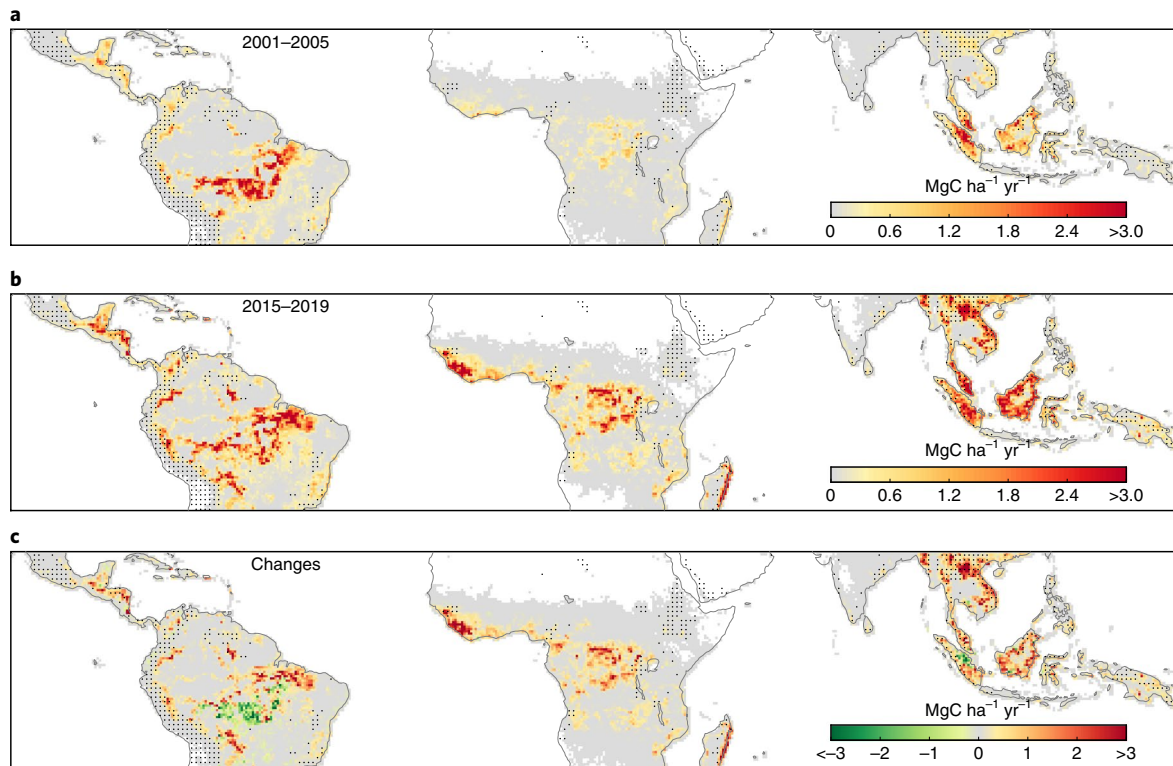


Fig. 2 | Spatial pattern of forest carbon loss across the tropics. a,b, Mean annual carbon loss during 2001–2005 (**a**) and 2015–2019 (**b**). **c**, Changes in mean annual carbon loss during 2015–2019 relative to the period 2001–2005. Black dots indicate mountain regions defined by Global Mountain Biodiversity Assessment (GMBA) inventory data; $1\text{MgC} = 10^{-9}\text{PgC}$. Forest carbon loss includes aboveground and (committed) belowground biomass carbon loss and (committed) soil organic carbon loss.

also plays an increasingly important role in forest carbon loss in this region. In Brazil, a substantial acceleration in forest carbon loss from small-scale agriculture ($24.3\text{TgCyr}^{-1}\text{decade}^{-1}$, $P < 0.05$) was partly opposed by a slight decrease in forest carbon loss from large-scale (commodity) agriculture ($-2.4\text{TgCyr}^{-1}\text{decade}^{-1}$; Table 1). Overall, total annual forest carbon loss in Brazil for the 19 yr period is the highest globally (373.0TgCyr^{-1} ; Table 1), far exceeding losses in any other country.

In contrast with tropical America, the increases in annual forest carbon loss in tropical Africa and Asia were continuous during the study period (Supplementary Fig. 2). In tropical Africa, the expansion of small-scale agriculture contributes to 34% of the doubling of tropical forest carbon loss worldwide. The increasing annual forest carbon loss in the Congo rainforest (Fig. 3f) relates to forests replaced by non-mechanized, small-scale, shifting agriculture, for example, in D. R. Congo, in neighbouring Angola and, to a lesser extent, in Cameroon^{28,29}. Often, these systems have evolved from traditional agriculture systems to hybrid forms using fire, shortened fallows, extended cultivation cycles and increasingly commercial crops³⁰. In tropical Asia, agricultural expansion also dominates (62%) the increase in forest carbon loss, contributing an 18% to the doubling of tropical carbon loss worldwide (Fig. 3d). However, losses in montane mainland and peninsular/maritime SEA are dissimilar (Fig. 3g,h). In the north of mainland SEA, commodity-driven forest carbon loss exhibits continuous increases that involve plantation rubber and vast expanses of maize grown for livestock feed³¹. Forestry activities associated with selective logging and smallholder farming are also responsible for considerable and increasing forest carbon loss²⁷. In peninsular/maritime SEA, forest conversion to oil-palm and rubber plantations³² makes up most forest carbon loss, which increased in magnitude in the region

during 2001–2011 before decreasing thereafter. Annual forest carbon loss in maritime SEA has not increased since 2010, in contrast to the increases occurring in the montane mainland SEA. This stabilization in maritime SEA may reflect the depletion of accessible forest following very long histories of exploitation²⁵. Despite stabilization in forest loss, Indonesia leads tropical Asia in annual forest carbon loss at 203.6TgCyr^{-1} , and Malaysia is the second, with 74.4TgCyr^{-1} (Table 1).

The fate of cleared lands

To further provide insights into the fate of converted lands, we visually interpret additional very-high-resolution (3–5 m) satellite imagery from Planet's Constellation to examine post-forest-loss land cover in 2020 from 1,000 randomly sampled GFC loss pixels where forests were replaced by agricultural lands (Methods and Supplementary Fig. 4a). This analysis shows that, across the tropics, ~30% of the lands transitioning to agriculture (either commodity or small-scale) began to regenerate as shrubland or forest by 2020 (Supplementary Fig. 4b). This level of agricultural 'abandonment', detectable as shrubland/forest in 2020, could result from land abandonment by farmers or from policies promoting restoration of forest land. It might also be, in part, associated with fallows and, therefore, a false signal of abandonment.

For tropical America, where commodity agriculture is the key driver of forest loss, more than 79% of the forest lands transitioning to agriculture in 2001–2019 remained agricultural lands in 2020 (Supplementary Fig. 4b). This finding suggests the possibility that the forests cleared were first logged, with farmers or ranchers later beginning agricultural activities and subsequently allowing some land to revert back to forest. In the Amazon, land speculation has been shown to leave the cleared lands unattended; poor planning,

Table 1 | Countries with the greatest forest carbon loss and associated drivers across the tropics between 2001 and 2019 (top 20)

| Country | Trend (TgC yr ⁻¹ decade ⁻¹) | | | | |
|--------------------------------|--|-------------------------|----------|--------|-------|
| | Commodity agriculture | Small-scale agriculture | Forestry | Others | Total |
| D. R. Congo | 2.6* | 92.2* | 0.3* | 3.3* | 98.4* |
| Indonesia | 82.8* | 10.8* | 4.5* | 2.2 | 95.2 |
| Brazil | -2.4 | 24.3* | 4.8* | 5.6* | 46.9 |
| Laos | 11.4* | 5.1* | 16.4* | 0.2* | 33.1* |
| Malaysia | 19.3* | 1.0* | 5.7* | 0.2* | 28.2* |
| Madagascar | 0.8* | 21.6* | 0.1* | 0.1 | 23.0* |
| Bolivia | 15.1* | 4.6* | -0.1* | 1.1* | 22.8* |
| Vietnam | 10.6* | 2.5* | 7.6* | 0.3* | 21.2* |
| Myanmar | 6.2* | 5.2* | 8.8* | 0.2* | 20.9* |
| Peru | 3.8* | 15.5* | 0.0* | 1.3* | 20.5* |
| Liberia | 0.9* | 13.0* | 0.0* | 0.1* | 14.0* |
| Cambodia | 12.8* | 0.7* | 0.3* | 0.1* | 13.7* |
| Côte d'Ivoire | 0.4* | 13.1* | 0.0* | 0.0* | 13.4* |
| Guinea | 1.0* | 12.6* | 0.0* | 0.1* | 13.3* |
| Angola | 0.2* | 12.5* | 0.0* | 0.2* | 12.8* |
| Cameroon | 0.7* | 10.6* | 0.1* | 0.7* | 12.0* |
| China | 0.8* | 0.2* | 10.2* | 0.3* | 11.6* |
| Thailand | 3.8* | 1.6* | 5.8* | 0.1* | 11.2* |
| Mozambique | 0.0* | 10.4* | 0.1* | 0.1* | 10.6* |
| Mexico | 0.9* | 6.9* | 0.4* | 0.7* | 9.6* |
| Amount (TgC yr ⁻¹) | | | | | |
| Brazil | 260.4 | 78.5 | 25.6 | 8.5 | 373.0 |
| Indonesia | 171.0 | 20.2 | 9.3 | 3.0 | 203.6 |
| D. R. Congo | 3.7 | 112.5 | 0.4 | 3.6 | 120.2 |
| Malaysia | 64.2 | 1.3 | 8.4 | 0.3 | 74.4 |
| Bolivia | 25.8 | 11.6 | 0.4 | 2.7 | 40.5 |
| Colombia | 8.5 | 24.2 | 0.9 | 1.4 | 35.0 |
| Peru | 6.4 | 24.5 | 0.1 | 1.5 | 32.5 |
| Laos | 12.4 | 4.6 | 14.4 | 0.1 | 31.5 |
| Madagascar | 0.8 | 23.2 | 0.1 | 0.2 | 24.3 |
| Vietnam | 13.0 | 3.1 | 7.2 | 0.3 | 23.5 |
| Mexico | 2.2 | 17.1 | 1.1 | 1.1 | 21.5 |
| Myanmar | 7.3 | 5.1 | 8.5 | 0.3 | 21.1 |
| Cambodia | 19.0 | 0.7 | 0.6 | 0.2 | 20.5 |
| China | 0.7 | 0.2 | 18.6 | 0.4 | 20.0 |
| Thailand | 6.1 | 2.4 | 8.0 | 0.2 | 16.7 |
| Côte d'Ivoire | 0.9 | 15.6 | 0.1 | 0.0 | 16.6 |
| Mozambique | 0.0 | 15.0 | 0.1 | 0.2 | 15.3 |
| Angola | 0.2 | 14.5 | 0.0 | 0.5 | 15.2 |
| Paraguay | 14.1 | 0.5 | 0.1 | 0.2 | 14.8 |
| Venezuela | 1.5 | 9.9 | 0.6 | 1.2 | 13.2 |

Gross forest carbon loss in these 20 countries accounts for 78% of the increase in tropical forest carbon loss and 83% of the total amount of the loss; 1 TgC is equivalent to 10⁻³ PgC. Forest carbon loss includes aboveground and (committed) belowground biomass carbon loss and (committed) soil organic carbon loss. *Statistically significant trend at $P < 0.05$.

financial shortage and illegal settlement have also forced farmers to abandon cultivated lands, leading to vegetation regrowth³³. For tropical Africa, where small-scale agriculture (often in the form of

shifting cultivation practices) is the dominant activity on formerly forested lands, the proportion remaining as agriculture in 2020 is smaller for areas where forest loss occurred between 2001–2005 (34%) compared with those where the loss occurred in 2015–2019 (57%). This difference suggests either an intensification of agriculture or a reduction in fallow length within shifting agriculture in this region. In tropical Asia, half of the cleared lands between 2001 and 2005 were not in agricultural use in 2020, but only ~20% of the lands cleared between 2015 and 2019 regenerated. The lower rate of abandonment of the more recently converted patches may possibly reflect an increasing percentage of clearing to support commodity agriculture³⁴. Overall, the high rate of abandonment of converted agricultural lands to regenerate suggests a waste of agricultural conversion, a situation that should be considered in land-use modelling.

Discussion

This study provides high-spatiotemporal-resolution quantification and attribution of forest carbon loss across the tropics, allowing new insights on the role of land-cover change^{35,36}. High-resolution satellite images help identify small-scale forest loss events and avoid some offsetting of forest losses by gains at a coarser pixel level^{12,14}. In coarse-resolution assessments, small-scale and/or partial forest loss is usually considered to be degradation¹² and, therefore, could be mapped inaccurately for carbon loss assessments. High-resolution satellite data also highlight the role of roads in providing access and, consequently, exploitation of formerly undisturbed forest resources, as documented in the Amazon for several years³⁷. Increasingly, forest carbon loss has occurred along road corridors in the Congo basin and SEA countries, including Laos^{38,39}. Rivers also provide access to forests and allow transport of forest and agriculture products downstream⁴⁰. The pervasive presence and acceleration of forest losses along roads and rivers in Amazon basin, the Congo basin and SEA (Supplementary Fig. 3) indicate that the frontier of forest loss has been carved deep into previously intact forests.

Our aboveground carbon loss estimate is comparable to previous assessments (Supplementary Table 1), yet with differences that originate, in part, from differences in methodology and input data, in the study period, and in the extent of tropical regions included. While other studies^{7,9,12,20,22} did not report carbon losses from belowground biomass and soils, our inclusion of these two components as committed loss terms increases the average forest carbon loss by 38% in our assessment. Further, our estimates of forest carbon loss should be more robust as we use an unbiased stratified random-sample approach and correct the mismatches of spatial resolution between forest loss (30 m) and carbon density maps (500–1,000 m) (ref. ⁴¹), reducing uncertainties in quantifying forest carbon loss. The stratified random-sample approach is independent of the change detection method in the GFC data, thereby reducing the likelihood of producing erroneous results during mapping^{16,17}. Importantly, our assessment identifies more forest loss in the mountains than have previous assessments, where land-clearing tends to occur in smaller patches that are not fully detectable by coarse-resolution images^{6,31,42}.

Further, the estimated trend in carbon loss from forest conversion to agriculture is positive (Supplementary Fig. 5), which differs from the flat or decreasing trend of gross sources calculated by three bookkeeping models used in the assessments of the global carbon budget¹. These bookkeeping models are forced by statistical data of national forest area or a model of agricultural area expansion⁴³ and may not capture spatial patterns of deforestation and impacted biomass carbon stocks. However, the gross carbon source of bookkeeping models¹ has a higher absolute value than our satellite-based results, probably because bookkeeping models include a simple account of forest degradation losses (based on harvest) whereas this carbon loss/recovery process is not included in our study. Further, bookkeeping models assume areas of shifting agriculture and a

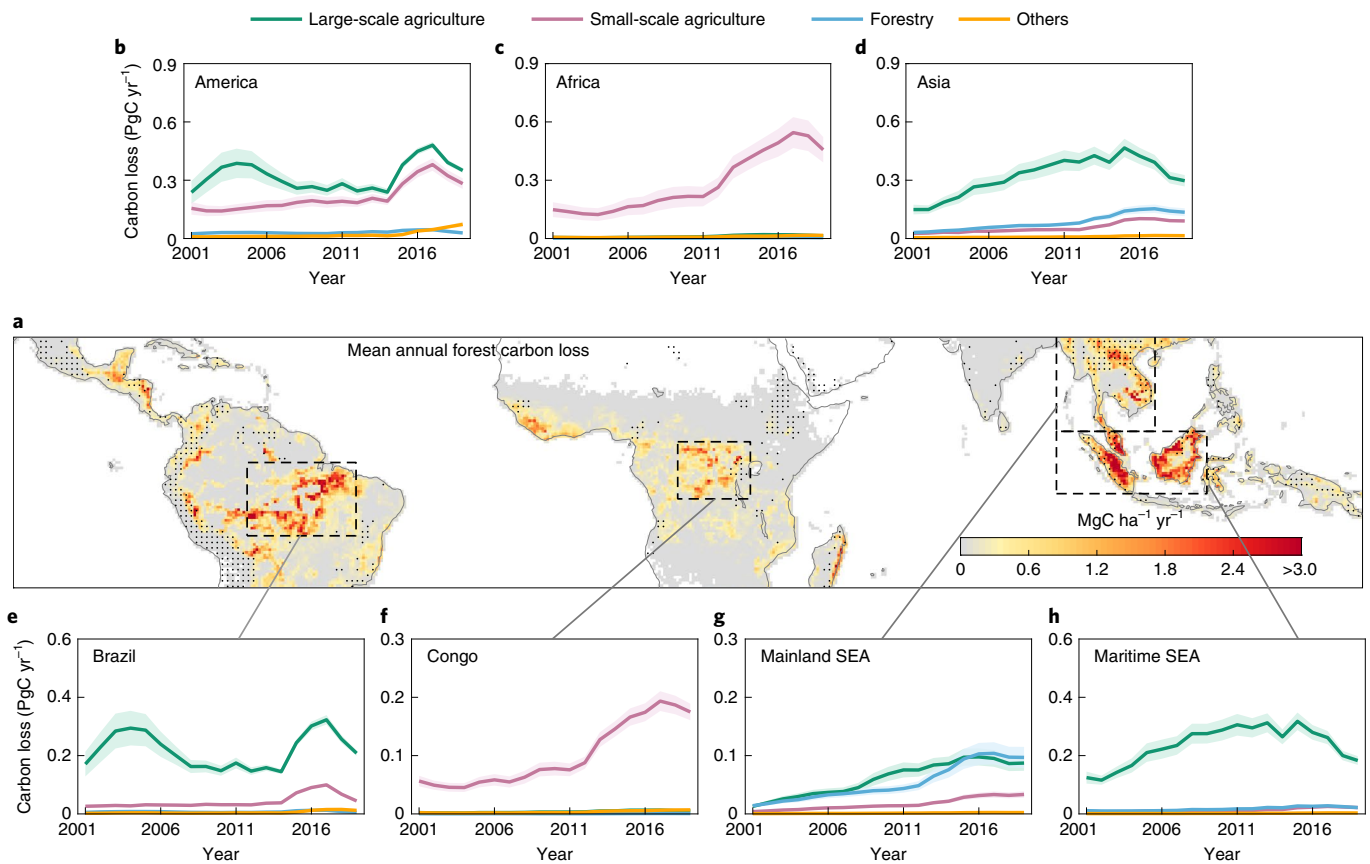


Fig. 3 | Regional forest carbon loss and its drivers across the tropics during 2001–2019. **a**, Spatial pattern of mean annual carbon loss. Black dots indicate mountain regions defined by G MBA inventory data. **b–h**, Trajectory of carbon loss resulting from different drivers in tropical America (**b**), tropical Africa (**c**), tropical Asia (**d**), Brazil (**e**), Congo basin (**f**), mainland SEA (**g**) and maritime SEA (**h**). The shaded area represents the s.d. estimated by four carbon density maps. Forest carbon loss includes aboveground and (committed) belowground biomass carbon loss and (committed) soil organic carbon loss.

residence time for this cultivation practice, whereas shifting agriculture is explicitly included in the satellite data that we analysed.

Concerning the uncertainties in our study, we estimated committed losses of belowground biomass carbon and SOC that do not fully represent the immediate emissions. Here, ‘committed’ means that we estimated the equilibrium value of carbon pools long after conversion, although some belowground vegetative biomass carbon and SOC would not be immediately lost (or emitted to the atmosphere) after forest removal. Dead aboveground biomass may be transferred to other carbon pools (for example, retaining in wood products¹² or decaying as slash), and belowground biomass may be retained in the soil and decay over time. The dynamics of these pools could be calculated in future studies using bookkeeping models and decay functions. Yet, our assumption of committed loss does not affect the long-term trend in annual forest carbon loss¹². Further, we used static biomass maps, which assume that the forest biomass does not change over time. Although earlier work tried to quantify forest biomass changes using annual biomass maps (that are not publicly available, to our knowledge)¹², these maps have uncertainties and give a biomass change inconsistent with higher-resolution GFC data in some regions⁴¹. Thus, we used four biomass maps (Methods) to quantify the uncertainty of forest carbon stocks⁴⁴. Considering the marginally small annual changes relative to total forest carbon stocks across the tropics⁴⁵, this assumption of static forest biomass does not question the doubling of the forest carbon loss. Further studies are required to map and quantify annual forest biomass change using more in situ biomass and lidar observations, as well as high-resolution satellite data. Overall, these uncertainties

are unlikely to impact our finding of the doubling of tropical carbon loss based on vegetative biomass and SOC changes immediately after forest removal.

The doubling of tropical forest carbon loss in the second decade of the twenty-first century demonstrates a failure to halve tropical deforestation rates by 2020 as committed under the 2014 New York Declaration on Forests²⁰. Our work demonstrates the immense challenge posed by the Glasgow Leaders’ Declaration on Forests and Land Use, which pledges to halt forest loss in less than a decade⁴⁶. Acceleration in tropical forest loss also casts doubt on the likelihood of achieving the carbon emission reduction target by 2030⁴⁷, making it more challenging to limit global warming to below 2 °C by the end of this century. Our findings highlight the importance of monitoring deforestation trends and imply an urgent need to reduce forest loss. We advocate that tropical nations put forward sustainable land management strategies and policies to effectively reduce forest carbon loss for climate change mitigation, which must include efficient and legal strategies to produce commodities and food without compromising tropical forests.

Methods

Global map of forest cover change and its validation. We use a high-resolution map of global forest cover change¹⁵ (annual intervals at 30 m spatial resolution; version 1.7) to quantify forest loss across the tropics. The GFC dataset maps where and when forests were converted (naturally and anthropogenically) from 2001 to 2019. Trees are defined as all vegetation taller than 5 m in height, and forests are defined with a tree canopy threshold of at least 30%. The definition of forests includes plantations and tree crops such as oil palm. Forest loss is the mortality or removal of all tree cover within a pixel.

Our study uses the v.1.7 product that spans the period 2001–2019 for the analysis. Different methods are used for detecting forest cover loss in two periods (2001–2010 and 2011–2019). This change in detection method as well as in satellite data (Landsat 7 and Landsat 8) might result in inconsistencies of data during the two periods. Therefore, we perform an independent assessment of the v.1.7 product throughout the study period (2001–2019) using stratified random-sample reference data. We randomly sample 18,000 pixels, a much larger sample population than the assessment of the original product (v.1.0, 628 pixels across the tropics; ref. ¹⁵), and visually interpret forest loss using Landsat imagery. Specifically, we randomly select 50 path/row locations (World Reference System II) of Landsat imagery in each tropical continent (150 path/row locations in total in the three tropical continents; Supplementary Fig. 6). For each path/row location, we randomly select 20 loss pixels and 10 non-loss pixels in each period of 2001–2005, 2006–2010, 2011–2014 and 2015–2019, with total sampling pixels of ~18,000 ((20 loss + 10 non-loss) × 50 path/row locations × 4 periods × 3 continents). Our study compares the increase in forest carbon loss from the start (~2001) to the end (~2019) of the study period. Thus, we divided the whole 19 yr study period into four subperiods (2001–2005, 2006–2010, 2011–2014 and 2015–2019), with the first five years considered as the start period and the last five years considered as the end period for the comparison. Some path/row locations do not have 20 loss pixels in a specific period; for example, there is no loss detected in some locations of the Sahara. Therefore, we sample 11,198 loss pixels and 6,000 non-loss pixels (Supplementary Data). Finally, we download time-series Landsat imagery covering 1999–2020 to visually interpret these pixels as reference data.

Following the suggestion of Global Forest Watch¹⁹ and per best practice guidance of ref. ¹⁸, we use a stratified random-sample approach for area estimation, which is independent of the method and satellite changes in the GFC data. The sampling reference data (Supplementary Data) are used to estimate loss area:

$$p_{hi} = w_h \frac{\sum_{j=1}^{150} n_{hij} \times A_{hi}}{\sum_{j=1}^{150} n_{hj} \times A_j} \quad (1)$$

where p_{hi} is the stratified random-sample estimated area for GFC map class h that is classified as reference class i ; w_h is the proportion of the total area GFC map class h ; n_{hij} is the number of pixels in GFC map class h that is classified as reference class i in j th Landsat path/row location; n_{hj} is the total number of pixels in GFC map class h in j th Landsat path/row location; A_{hi} is the total area in GFC map class h in i th Landsat path/row location; and A_j is the total land area of j th Landsat path/row location.

We then calculate the error matrix, which includes overall accuracy (OA), user's accuracy (UA) and producer's accuracy (PA), as follows:

$$OA = \sum_{h=1}^H p_{hh} \quad (2)$$

$$UA_h = \frac{p_{hh}}{p_h} \quad (3)$$

$$PA_j = \frac{p_{jj}}{p_j} \quad (4)$$

where UA_h is the UA for stratum h ; p_h and p_j are the total area in stratum h and j , respectively; and PA_j is the PA in stratum j .

Using the preceding equations, we estimate OA, UA and PA in the four periods (Supplementary Table 2). In general, OAs are >99%, UAs are >88% and PAs are >72% in each period. The stratified random-sample approach for area estimation is considered the most robust method to investigate loss trends in GFC product and can avoid inconsistencies of the dataset due to changes in detection model and satellite sensors¹⁹. Our results show that the forest loss from the stratified random-sample approach is similar to GFC mapped loss, both of which show a consistent increase during the four periods of 2001–2019 (Fig. 1a), confirming the increasing forest carbon loss across the tropics during the early twenty-first century.

Forest carbon stocks. We estimate forest (aboveground and belowground) biomass carbon losses by co-locating GFC loss data with corresponding biomass data.

Forest biomass maps are not universally reliable, owing to uncertainties and some degree of bias. We use four biomass maps to quantify forest carbon stocks, which helps reduce the uncertainties and bias⁴¹. The four maps were developed by refs. ^{9,48,49,20} and are hereafter referred to as 'Baccini', 'Saatchi', 'Avitabile' and 'Zarin' maps, respectively. The Baccini map, derived from Moderate Resolution Imaging Spectroradiometer (MODIS) data, presents aboveground live woody biomass (AGB) across the tropics at 500 m spatial resolution. The Saatchi map, also derived from MODIS data, presents total forest carbon stocks at 1 km spatial resolution across the tropics. The Avitabile map, integrated from the Baccini and Saatchi

maps, shows AGB at 1 km resolution across the tropics. The Zarin map, derived from Landsat data, presents AGB across the globe at 30 m resolution.

Belowground root biomass (BGB) data are sparse because measurements of BGB are time consuming, laborious and technically challenging⁴⁰. Thus, we calculate BGB (in Mg ha^{-1} biomass) from AGB maps (Baccini, Avitabile and Zarin) using an empirical model at the pixel level⁵¹:

$$BGB = 0.489 \times AGB^{0.89} \quad (5)$$

Total forest biomass is calculated as the sum of AGB and BGB. Finally, total forest carbon stocks (MgCha^{-1}) in live woody forest are estimated as 50% of total biomass^{20,50}. The Saatchi map provides total forest carbon stocks rather than AGB. The total forest carbon stocks are calculated from AGB using the same method mentioned in the preceding⁴⁰. Thus, we estimate AGB and BGB from total forest carbon stocks in the Saatchi map using the preceding method to separate aboveground and belowground parts of forest carbon stocks.

There are inconsistencies in the MODIS-derived biomass maps (Baccini, Saatchi and Avitabile) and Landsat-derived GFC data⁴¹, which may underestimate forest carbon loss by the three coarse forest biomass maps (Supplementary Fig. 7). The Zarin map is derived from Landsat data and considers tree cover using GFC data, and tree loss can be co-located with the corresponding biomass²⁰, indicating the inconsistencies of the Zarin map and GFC. Therefore, to correct the three biomass maps with coarse resolution and reduce the inconsistencies, we resample the Zarin map from 30 m to 500 m (the resolution of the Baccini map) and 1 km (the resolutions of the Avitabile and Baccini maps) and calculate forest carbon loss using the two resampled biomass maps. We then estimate the ratios of forest carbon loss derived from the 30 m biomass map to the forest carbon loss derived from resampled biomass maps in each GFC tile ($10^\circ \times 10^\circ$). The ratios are then used as a scale factor to correct the three biomass maps (Baccini, Saatchi and Avitabile). For the resampling, forest carbon density at 500 m or 1 km is averaged from all 30 m pixels in the corresponding locations.

Soil organic carbon stocks. Deforestation not only causes forest biomass carbon loss, but also results in loss of SOC¹⁰. We calculate SOC loss at 0–30 cm soil depth as:

$$SOC_{\text{loss}} = OCS \times \theta \quad (6)$$

where SOC_{loss} is SOC loss resulting from forest loss measured in MgCha^{-1} , OCS is SOC stocks at 0–30 cm depth measured in MgCha^{-1} and θ is the SOC loss rate.

We obtain SOC stocks at 0–30 cm depth from SoilGrids (version 2.0), created by the International Soil Reference and Information Centre⁵². SOC stocks are calculated using a calibrated quantile random forest model at a spatial resolution of 250 m. We further resample the data from 250 m to 30 m using the nearest-neighbour method to match the scale of forest cover loss data.

SOC loss rate is affected predominantly by land-use types following forest loss and tree species⁵³. The loss rate data are compiled from a previous meta-analysis, which summarizes the rate of SOC loss resulting from forest loss over the tropics⁵⁰. SOC losses resulting from primary and secondary forest loss differ (Supplementary Table 3). We use a map of primary humid tropical forests in 2001 developed by ref. ⁵⁴ to classify primary and secondary forests. The land covers following forest loss are determined according to the driver of forest loss (see Drivers of forest carbon loss). The spatial resolution of the SOC data is coarse compared with GFC data, which may result in inconsistencies in the calculation. However, as SOC loss resulting from forest loss accounts for a small proportion of total forest carbon loss (8%), we ignore the potential inconsistencies.

Drivers of forest carbon loss. We determine drivers of tree-cover loss using the dataset generated by ref. ²⁷. This dataset shows the dominant driver of tree-cover loss at each 10 km grid cell for 2001–2019. There are five categories of drivers of tree-cover loss: commodity-driven deforestation, defined as permanent and/or long-term clearing of trees to other land uses (for example, commodity croplands), shifting agriculture, forestry, wildfire and urbanization. Commodity-driven deforestation, shifting agriculture and forestry dominate tropical forest loss²⁷. Thus, wildfire and urbanization are combined and categorized as 'others'. In tropical Africa, spatial patterns of commodity-driven deforestation are almost similar to that of shifting agriculture, as pointed out by ref. ²⁷, resulting in large uncertainties in separating commodity agriculture from shifting agriculture. Since commodity-driven deforestation is usually for large-scale agricultural plantations, we treat commodity-driven deforestation as loss for large-scale agriculture. Because shifting agriculture is usually smallholder and/or patchy farming systems, we term shifting agriculture as small-scale agriculture, which may include commodity agriculture with similar spatial patterns to shifting agriculture in some regions such as tropical Africa. The driver data are created using decision-tree models trained by ~5,000 high-resolution Google Earth imagery cells, showing overall accuracy of $89 \pm 3\%$ from a separate validation of more than 1,500 randomly selected cells. We resample the data from 10 km resolution to 30 m using the nearest-neighbour method to match the scale of forest cover loss data.

Interpretation of post-forest-loss land covers in 2020. We collect cloudless and very-high-resolution satellite imagery in 2020 from Planet to determine the fate of

the agriculture-driven forest loss during 2001–2019. Planet provides two products, RapidEye (at a spatial resolution of 5 m) and Doves (at a spatial resolution of 3 m; 4-band PlanetScope Scene). We randomly sample 500 pixels that show forest loss owing to agriculture expansion during 2001–2005 and 500 pixels that show forest loss owing to agriculture expansion during 2015–2019, then check cloudless satellite imagery in 2020 to visually interpret the land cover of each sampled pixel in 2020. We classify three types of land cover: agricultural land, forests/shrubland and others (Supplementary Fig. 4). Rubber and oil-palm plantations are classified as agricultural lands.

Uncertainty and methods for analysis. We use committed emissions of forest carbon, even though some of this carbon will be lost only in later years or transited to other carbon pools or stored as wood products¹². Forest carbon loss is defined as gross carbon loss due to forest removal (as indicated by GFC product), including (aboveground and belowground) forest biomass carbon and SOC losses. We calculate only the gross loss of forest carbon stocks while gain of carbon via reforestation and afforestation is not considered.

We first estimate reference sample-based forest loss area using sample data:

$$AS_j = AM_j \sum_{h=1}^H p_{hj} \quad (7)$$

where AS_j and AM_j are reference sample-based forest loss areas and mapped forest loss areas in stratum j , respectively.

To estimate forest carbon loss (aboveground, belowground and soil carbon) using sample-based forest loss area, we apply a 'stratify and multiply' approach^{21,22} by assigning mean forest carbon density for each stratum. Aboveground and belowground forest carbon losses are estimated using four biomass maps (Baccini, Saatchi, Avitabile and Zarin), and we report ensemble mean \pm s.d. from the four maps as our best estimate.

Mountain forest carbon loss at different elevations is calculated by overlaying mountain polygon from the Global Mountain Biodiversity Assessment inventory⁵ (version 1.2) and the 30 m ASTER Global Digital Elevation Model³⁶ (version 3).

Although our validation shows that the GFC (v.1.7) product could accurately map forest loss, we cannot reduce the omission and commission errors. In addition, the accuracy of the disturbance year is 75.2%, with 96.7% of the disturbance occurring within one year before or after the estimated disturbance year in GFC product¹⁵. Therefore, we calculate 3 yr moving averages of annual forest and related carbon losses for time-series analysis, following the suggestion of the Global Forest Watch¹⁹ and refs.^{28,38}. We use a non-parametric Theil–Sen estimator regression method³³ to detect trends in time-series results and test the significance of the trend by Mann–Kendall test²⁷.

Reporting Summary. Further information on research design is available in the Nature Research Reporting Summary linked to this article.

Data availability

The global map of forest cover loss is available at https://earthenginepartners.appspot.com/science-2013-global-forest/download_v1.7.html. The ASTER elevation data are available at <https://earthdata.nasa.gov/>. The GMBA inventory is available at https://ilias.unibe.ch/goto_ilias3_unibe_cat_1000515.html. The map describing the drivers of forest loss is available at <https://data.globalforestwatch.org/datasets/tree-cover-loss-by-dominant-driver>. The four biomass maps (Avitabile, Baccini, Saatchi and Zarin) are available at <http://lucid.wur.nl/datasets/high-carbon-ecosystems>, https://developers.google.com/earth-engine/datasets/catalog/WHRC_biomass_tropical, https://gfw2-data.s3.amazonaws.com/forest_cover/zip/tropical_forest_carbon_stocks.tif.aux.zip and https://data.globalforestwatch.org/datasets/3e8736c8866b458687e00d40c9f00bce_0/about, respectively. Soil carbon stocks are available at <https://www.isric.org/explore/soilgrids>. The primary humid tropical forest map is available at <https://glad.umd.edu/dataset/primary-forest-humid-tropics>. The Planet very-high-resolution satellite imagery is available at www.planet.com. Time-series Landsat imagery is available at <https://earthexplorer.usgs.gov/>. All datasets are also available upon request from Z. Zeng.

Code availability

The scripts used to generate all the results are MATLAB (R2020a). Analysis scripts are available on request from Z. Zeng.

Received: 2 September 2021; Accepted: 19 January 2022;

Published online: 28 February 2022

References

- Friedlingstein, P. et al. Global carbon budget 2021. Preprint at *Earth Syst. Sci. Data Discuss.* <https://doi.org/10.5194/essd-2021-386> (2021).
- Arnell, A. et al. Historical carbon dioxide emissions caused by land-use changes are possibly larger than assumed. *Nat. Geosci.* **10**, 79–84 (2017).
- Piao, S. et al. Lower land-use emissions responsible for increased net land carbon sink during the slow warming period. *Nat. Geosci.* **11**, 739–743 (2018).
- Gasser, T. et al. Historical CO₂ emissions from land use and land cover change and their uncertainty. *Biogeosciences* **17**, 4075–4101 (2020).
- Friedlingstein, P. et al. Global carbon budget 2019. *Earth Syst. Sci. Data* **11**, 1783–1838 (2019).
- Zeng, Z. et al. Highland cropland expansion and forest loss in Southeast Asia in the twenty-first century. *Nat. Geosci.* **11**, 556–562 (2018).
- Harris, N. L. et al. Baseline map of carbon emissions from deforestation in tropical regions. *Science* **336**, 1573–1576 (2012).
- Harris, N. L. et al. Global maps of twenty-first century forest carbon fluxes. *Nat. Clim. Change* **11**, 234–240 (2021).
- Baccini, A. et al. Estimated carbon dioxide emissions from tropical deforestation improved by carbon-density maps. *Nat. Clim. Change* **2**, 182–185 (2012).
- Veldkamp, E. et al. Deforestation and reforestation impacts on soils in the tropics. *Nat. Rev. Earth Environ.* **1**, 590–605 (2020).
- Bonan, G. B. Forests and climate change: forcings, feedbacks, and the climate benefits of forests. *Science* **320**, 1444–1449 (2008).
- Baccini, A. et al. Tropical forests are a net carbon source based on aboveground measurements of gain and loss. *Science* **358**, 230–234 (2017).
- Brinck, K. et al. High resolution analysis of tropical forest fragmentation and its impact on the global carbon cycle. *Nat. Commun.* **8**, 14855 (2017).
- Mitchard, E. T. A. The tropical forest carbon cycle and climate change. *Nature* **559**, 527–534 (2018).
- Hansen, M. C. et al. High-resolution global maps of 21st-century forest cover change. *Science* **342**, 850–853 (2013).
- Wernick, I. K. et al. Quantifying forest change in the European Union. *Nature* **592**, E13–E14 (2021).
- Palahi, M. et al. Concerns about reported harvests in European forests. *Nature* **592**, E15–E17 (2021).
- Olofsson, P. et al. Good practices for estimating area and assessing accuracy of land change. *Remote Sens. Environ.* **148**, 42–57 (2014).
- Weisse, M. & Potapov, P. Assessing trends in tree cover loss over 20 years of data. *Global Forest Watch* <https://www.globalforestwatch.org/blog/data-and-research/tree-cover-loss-satellite-data-trend-analysis/> (2021).
- Zarin, D. J. et al. Can carbon emissions from tropical deforestation drop by 50% in 5 years? *Glob. Change Biol.* **22**, 1336–1347 (2016).
- Goetz, S. J. et al. Mapping and monitoring carbon stocks with satellite observations: a comparison of methods. *Carbon Balance Manage.* **4**, 2 (2009).
- Tyukavina, A. et al. Aboveground carbon loss in natural and managed tropical forests from 2000 to 2012. *Environ. Res. Lett.* **10**, 074002 (2015).
- Feng, Y. et al. Upward expansion and acceleration of forest clearance in the mountains of Southeast Asia. *Nat. Sustain.* **4**, 892–899 (2021).
- Spracklen, D. V. & Righelato, R. Tropical montane forests are a larger than expected global carbon store. *Biogeosciences* **11**, 2741–2754 (2014).
- Curran, L. M. et al. Lowland forest loss in protected areas of Indonesian Borneo. *Science* **303**, 1000–1003 (2004).
- Qin, Y. et al. Carbon loss from forest degradation exceeds that from deforestation in the Brazilian Amazon. *Nat. Clim. Change* **11**, 442–448 (2021).
- Curtis, P. G., Slay, C. M., Harris, N. L., Tyukavina, A. & Hansen, M. C. Classifying drivers of global forest loss. *Science* **361**, 1108–1111 (2018).
- Tyukavina, A. et al. Congo basin forest loss dominated by increasing smallholder clearing. *Sci. Adv.* **4**, eaat2993 (2018).
- Wallenfang, J. et al. Impact of shifting cultivation on dense tropical woodlands in southeast Angola. *Trop. Conserv. Sci.* **8**, 863–892 (2015).
- Van Vliet, N. et al. Trends, drivers and impacts of changes in swidden cultivation in tropical forest–agriculture frontiers: a global assessment. *Glob. Environ. Change* **22**, 418–429 (2012).
- Zeng, Z., Gower, D. B. & Wood, E. F. Accelerating forest loss in Southeast Asian Massif in the 21st century: a case study in Nan Province, Thailand. *Glob. Change Biol.* **24**, 4682–4695 (2018).
- Austin, K. G. et al. What causes deforestation in Indonesia? *Environ. Res. Lett.* **14**, 024007 (2019).
- Hanbury, S. Brazil scientists map forest regrowth keeping Amazon from collapse: study. *Mongabay Environmental News* <https://news.mongabay.com/2020/12/brazil-scientists-map-forest-regrowth-keeping-amazon-from-collapse-study> (2020).
- Austin, K. G. et al. Trends in size of tropical deforestation events signal increasing dominance of industrial-scale drivers. *Environ. Res. Lett.* **12**, 054009 (2017).
- Ramo, R. et al. African burned area and fire carbon emissions are strongly impacted by small fires undetected by coarse resolution satellite data. *Proc. Natl Acad. Sci. USA* **118**, e2011160118 (2021).
- Song, X.-P. et al. Global land change from 1982 to 2016. *Nature* **560**, 639–643 (2018).
- Barber, C. P., Cochrane, M. A., Souza, C. M. Jr & Laurance, W. F. Roads, deforestation, and the mitigating effect of protected areas in the Amazon. *Biol. Conserv.* **177**, 203–209 (2014).
- Kleinschroth, F. et al. Road expansion and persistence in forests of the Congo basin. *Nat. Sustain.* **2**, 628–634 (2019).

39. Phompila, C., Lewis, M., Ostendorf, B. & Clarke, K. Forest cover changes in Lao tropical forests: physical and socio-economic factors are the most important drivers. *Land* **6**, 23 (2017).
40. In pictures: Illegal logging in Peru. *BBC News* <https://www.bbc.com/news/world-latin-america-28926270> (2014).
41. Hansen, M. C., Potapov, P. & Tyukavina, A. Comment on “Tropical forests are a net carbon source based on aboveground measurements of gain and loss”. *Science* **363**, eaar3629 (2019).
42. Zeng, Z. et al. Deforestation-induced warming over tropical mountain regions regulated by elevation. *Nat. Geosci.* **14**, 23–29 (2021).
43. Hurtt, G. C. et al. Harmonization of global land use change and management for the period 850–2100 (LUH2) for CMIP6. *Geosci. Model Dev.* **13**, 5425–5464 (2020).
44. Fan, L. et al. Satellite-observed pantropical carbon dynamics. *Nat. Plants* **5**, 944–951 (2019).
45. Xu, L. et al. Changes in global terrestrial live biomass over the 21st century. *Sci. Adv.* **7**, eabe9829 (2021).
46. Glasgow leaders' declaration on forests and land use. *UN Climate Change Conference* <https://ukcop26.org/glasgow-leaders-declaration-on-forests-and-land-use/> (2021).
47. Admiraal, A. et al. *Assessing Intended Nationally Determined Contributions to the Paris Climate Agreement—What are the Projected Global and National Emission Levels for 2025–2030?* Report No. PBL 1879 (PBL, 2015); <http://www.pbl.nl/en/publications/assessing-intended-nationally-determined-contributions-to-the-paris-climate-agreement>
48. Saatchi, S. S. et al. Benchmark map of forest carbon stocks in tropical regions across three continents. *Proc. Natl Acad. Sci. USA* **108**, 9899–9904 (2011).
49. Avitabile, V. et al. An integrated pan-tropical biomass map using multiple reference datasets. *Glob. Change Biol.* **22**, 1406–1420 (2016).
50. Don, A., Schumacher, J. & Freibauer, A. Impact of tropical land-use change on soil organic carbon stocks—a meta-analysis. *Glob. Change Biol.* **17**, 1658–1670 (2011).
51. Mokany, K., Raison, R. J. & Prokushkin, A. S. Critical analysis of root:shoot ratios in terrestrial biomes. *Glob. Change Biol.* **12**, 84–96 (2006).
52. Hengl, T. et al. SoilGrids250m: global gridded soil information based on machine learning. *PLoS ONE* **12**, e0169748 (2017).
53. Sen, P. K. Estimates of the regression coefficient based on Kendall's tau. *J. Am. Stat. Assoc.* **63**, 1379–1389 (1968).
54. Turubanova, S. et al. Ongoing primary forest loss in Brazil, Democratic Republic of the Congo, and Indonesia. *Environ. Res. Lett.* **13**, 074028 (2018).
55. Körner, C. et al. A global inventory of mountains for bio-geographical applications. *Alp. Bot.* **127**, 1–15 (2016).
56. Tachikawa, T., Hato, M., Kaku, M. & Iwasaki, A. Characteristics of ASTER GDEM version 2. In *Proc. Geoscience and Remote Sensing Symposium* 3657–3660 (IEEE, 2011).
57. Mann, H. B. Nonparametric tests against trend. *Econometrica* **13**, 245–259 (1945).

Acknowledgements

This study was supported by the National Natural Science Foundation of China (grants no. 42071022, 41861124003 and 41890852) and the start-up fund provided by Southern University of Science and Technology (no. 29/Y01296122). We thank Hansen/UMD/Google/USGS/NASA for providing the high-resolution forest change data; NASA and Japan's Ministry of Economy, Trade and Industry for providing the elevation data; Körner for providing the GMBIA inventory; Avitabile, Baccini, Saatchi and Zarin/GFW for providing the aboveground biomass density maps; Curtis/GFW for providing forest loss driver maps; SoilGrids/ISRIC for providing soil organic carbon data; Turubanova/UMD for providing primary humid tropical forest maps; and Planet for providing very-high-resolution satellite imagery. We thank S. Hu, S. Liang, Y. Liu, Y. Liu, J. Zou and B. Zeng for validating the GFC product via high-resolution satellite image interpretation.

Author contributions

Z.Z. and T.D.S. designed the research; Y.F. performed the analysis; Y.F., Z.Z., T.D.S. and A.D.Z. wrote the draft. All authors contributed to the interpretation of the results and the writing of the paper.

Competing interests

The authors declare no competing interests.

Additional information

Supplementary information The online version contains supplementary material available at <https://doi.org/10.1038/s41893-022-00854-3>.

Correspondence and requests for materials should be addressed to Zhenzhong Zeng, Ji Chen or Chunmiao Zheng.

Peer review information *Nature Sustainability* thanks Rico Fischer, Sharif Mukul and Pontus Olofsson for their contribution to the peer review of this work.

Reprints and permissions information is available at www.nature.com/reprints.

Publisher's note Springer Nature remains neutral with regard to jurisdictional claims in published maps and institutional affiliations.



Open Access This article is licensed under a Creative Commons Attribution 4.0 International License, which permits use, sharing, adaptation, distribution and reproduction in any medium or format, as long as you give appropriate credit to the original author(s) and the source, provide a link to the Creative Commons license, and indicate if changes were made. The images or other third party material in this article are included in the article's Creative Commons license, unless indicated otherwise in a credit line to the material. If material is not included in the article's Creative Commons license and your intended use is not permitted by statutory regulation or exceeds the permitted use, you will need to obtain permission directly from the copyright holder. To view a copy of this license, visit <http://creativecommons.org/licenses/by/4.0/>.

© The Author(s) 2022

Reporting Summary

Nature Portfolio wishes to improve the reproducibility of the work that we publish. This form provides structure for consistency and transparency in reporting. For further information on Nature Portfolio policies, see our [Editorial Policies](#) and the [Editorial Policy Checklist](#).

Statistics

For all statistical analyses, confirm that the following items are present in the figure legend, table legend, main text, or Methods section.

- | | |
|-------------------------------------|--|
| n/a | Confirmed |
| <input checked="" type="checkbox"/> | <input type="checkbox"/> The exact sample size (n) for each experimental group/condition, given as a discrete number and unit of measurement |
| <input checked="" type="checkbox"/> | <input type="checkbox"/> A statement on whether measurements were taken from distinct samples or whether the same sample was measured repeatedly |
| <input type="checkbox"/> | <input checked="" type="checkbox"/> The statistical test(s) used AND whether they are one- or two-sided <i>Only common tests should be described solely by name; describe more complex techniques in the Methods section.</i> |
| <input checked="" type="checkbox"/> | <input type="checkbox"/> A description of all covariates tested |
| <input type="checkbox"/> | <input checked="" type="checkbox"/> A description of any assumptions or corrections, such as tests of normality and adjustment for multiple comparisons |
| <input type="checkbox"/> | <input checked="" type="checkbox"/> A full description of the statistical parameters including central tendency (e.g. means) or other basic estimates (e.g. regression coefficient) AND variation (e.g. standard deviation) or associated estimates of uncertainty (e.g. confidence intervals) |
| <input type="checkbox"/> | <input checked="" type="checkbox"/> For null hypothesis testing, the test statistic (e.g. F , t , r) with confidence intervals, effect sizes, degrees of freedom and P value noted <i>Give P values as exact values whenever suitable.</i> |
| <input checked="" type="checkbox"/> | <input type="checkbox"/> For Bayesian analysis, information on the choice of priors and Markov chain Monte Carlo settings |
| <input checked="" type="checkbox"/> | <input type="checkbox"/> For hierarchical and complex designs, identification of the appropriate level for tests and full reporting of outcomes |
| <input checked="" type="checkbox"/> | <input type="checkbox"/> Estimates of effect sizes (e.g. Cohen's d , Pearson's r), indicating how they were calculated |

Our web collection on [statistics for biologists](#) contains articles on many of the points above.

Software and code

Policy information about [availability of computer code](#)

Data collection

Data analysis

For manuscripts utilizing custom algorithms or software that are central to the research but not yet described in published literature, software must be made available to editors and reviewers. We strongly encourage code deposition in a community repository (e.g. GitHub). See the Nature Portfolio [guidelines for submitting code & software](#) for further information.

Data

Policy information about [availability of data](#)

All manuscripts must include a [data availability statement](#). This statement should provide the following information, where applicable:

- Accession codes, unique identifiers, or web links for publicly available datasets
- A description of any restrictions on data availability
- For clinical datasets or third party data, please ensure that the statement adheres to our [policy](#)

The global map of forest cover loss is available at https://earthenginepartners.appspot.com/science-2013-global-forest/download_v1.7.html. The ASTER elevation data are available at <https://earthdata.nasa.gov/>. The GMBA inventory is available at https://ilias.unibe.ch/goto_ilias3_unibe_cat_1000515.html. The map describing the drivers of forest loss is available at <https://data.globalforestwatch.org/datasets/tree-cover-loss-by-dominant-driver>. The four biomass maps (Avitabile, Baccini, Saatchi, and Zarin) are available at <http://lucid.wur.nl/datasets/high-carbon-ecosystems>, https://developers.google.com/earth-engine/datasets/catalog/WHRC_biomass_tropical, https://gfw2-data.s3.amazonaws.com/forest_cover/zip/tropical_forest_carbon_stocks.tif.aux.zip, and https://data.globalforestwatch.org/datasets/3e8736c8866b458687e00d40c9f00bce_0/about, respectively. Soil carbon stocks are available at <https://www.isric.org/explore/soilgrids>. The primary humid tropical forest map is available at <https://glad.umd.edu/dataset/primary-forest-humid-tropics>. The Planet very-high-resolution

Field-specific reporting

Please select the one below that is the best fit for your research. If you are not sure, read the appropriate sections before making your selection.

Life sciences Behavioural & social sciences Ecological, evolutionary & environmental sciences

For a reference copy of the document with all sections, see [nature.com/documents/nr-reporting-summary-flat.pdf](https://www.nature.com/documents/nr-reporting-summary-flat.pdf)

Ecological, evolutionary & environmental sciences study design

All studies must disclose on these points even when the disclosure is negative.

| | |
|--------------------------|--|
| Study description | Using high-resolution forest loss data and forest carbon density data, this study investigated the trends and drivers of forest carbon loss over the tropics during 2001-2019. |
| Research sample | N.A. |
| Sampling strategy | N.A. |
| Data collection | N.A. |
| Timing and spatial scale | The data were between 2001-2019 at annual interval and 30m spatial resolution. |
| Data exclusions | N.A. |
| Reproducibility | N.A. |
| Randomization | N.A. |
| Blinding | N.A. |

Did the study involve field work? Yes No

Reporting for specific materials, systems and methods

We require information from authors about some types of materials, experimental systems and methods used in many studies. Here, indicate whether each material, system or method listed is relevant to your study. If you are not sure if a list item applies to your research, read the appropriate section before selecting a response.

Materials & experimental systems

- | n/a | Involvement in the study |
|-------------------------------------|--|
| <input checked="" type="checkbox"/> | <input type="checkbox"/> Antibodies |
| <input checked="" type="checkbox"/> | <input type="checkbox"/> Eukaryotic cell lines |
| <input checked="" type="checkbox"/> | <input type="checkbox"/> Palaeontology and archaeology |
| <input checked="" type="checkbox"/> | <input type="checkbox"/> Animals and other organisms |
| <input checked="" type="checkbox"/> | <input type="checkbox"/> Human research participants |
| <input checked="" type="checkbox"/> | <input type="checkbox"/> Clinical data |
| <input checked="" type="checkbox"/> | <input type="checkbox"/> Dual use research of concern |

Methods

- | n/a | Involvement in the study |
|-------------------------------------|---|
| <input checked="" type="checkbox"/> | <input type="checkbox"/> ChIP-seq |
| <input checked="" type="checkbox"/> | <input type="checkbox"/> Flow cytometry |
| <input checked="" type="checkbox"/> | <input type="checkbox"/> MRI-based neuroimaging |